Selection Effect in Dark Energy Survey Y1

Chiara Coviello

Supervisor: James Annis

Fermilab Summer School 2022

7 October 2022

Contents

Abstract

The discovery that the Universe expansion is accelerated poses one of the most profound mysteries in physics. Cosmic acceleration could be a sign of the fact that General Relativity breaks down on cosmological scales and has to be replaced, or it could arise from an unknown form of energy that currently dominates our Universe. That is what we call dark energy and in this case the problem moves to the discovery of its nature. Dark Energy Survey aims to study the nature of dark energy and to test General Relativity and cosmological models. The cluster analysis of the first run of DES leads to results which are incomparable with what other surveys have obtained. In particular it turns out that the matter density of the Universe is $\Omega_m = 0.179^{+0.031}_{-0.038}$, very different from the 0.3 value expected. In this work we build a procedure that can be followed in order to understand whether the solution of DES Y1 problem could be a selection effect or not.

1 Dark Energy

In this section we introduce what we refers to when we talk about dark energy.
We have to start from Friedmann equations, which are just the Einstein equation (that relates the curvature and so the geometry of the space-time (this information is inside the Einstein tensor $G_{\mu\nu}$) to the distribution of energy-matter within it (the energy-momentum tensor is $T_{\mu\nu}$)) evaluated in the FRWL metric, which is the metric of the Universe. Therefore -considering c=1; a(t): the scale factor of the Universe (that is where all the time dependence of the metric goes to, so it describes the Universe dynamics); k equals to 1 in the case of a spherical metric, to 0 in the case of a flat Universe and to -1 if we consider an hyperboloid metric- we have:

$$G_{\mu\nu} = 8\pi G T_{\mu\nu} \tag{1}$$

in

$$ds^2 = -dt^2 + a^2(t)\left[\frac{dr^2}{(1-kr^2)} + r^2(d\theta^2 + sin^2\theta d\phi^2)\right] \tag{2}$$

gives the two Friedmann equations:

$$\left(\frac{\dot{a}}{a}\right)^2 + \frac{k}{a^2} = \frac{8\pi G}{3}\rho \tag{3}$$

$$\frac{\ddot{a}}{a} = -\frac{4\pi G}{3}(\rho + 3p) \tag{4}$$

Now we observe that we can rewrite (3) by using the definition of the critical density:

$$\rho_{crit} \equiv \frac{3H^2}{8\pi G} \tag{5}$$

where $H(t) \equiv \frac{\dot{a}(t)}{a(t)}$ is the Hubble parameter, and $H(t_0) = 73.48 \pm 1.65\ km\, s^{-1}\, Mpc^{-1}$ is the expansion rate of the Universe at the present time. If we define the density parameter $\Omega \equiv \frac{\rho}{\rho_{crit}}$ and $\Omega_K \equiv -\frac{k}{a^2H^2}$ then (3) becomes:

$$-\Omega_K = \Omega - 1 \tag{6}$$

Equation (6) relates topological proprieties of the Universe to its energy density. We have that if $\Omega > 1$ then $k = 1$ and so we have a closed Universe; if $\Omega = 1$ then $k = 0$ and so we have a flat Universe and if $\Omega < 1$ then $k = -1$ and it implies an open Universe. It is important to notice the a-dependence of ρ (and so of Ω): considering the equation of state:

$$p = \omega\rho \tag{7}$$

and using the energy-momentum tensor conservation law:

$$\frac{\partial \rho}{\partial t} + 3\frac{\dot{a}}{a}(\rho + p) = 0 \tag{8}$$

we can find:

$$\rho \propto a^{-3(1+\omega)} \tag{9}$$

Since for cold dark matter $\omega = 0$ then $\Omega_M \propto a^{-3}$; for the radiation $\omega = 1/3$ and so $\Omega_R \propto a^{-4}$ and if we consider a fluid with $\omega = -1$ then $\Omega = const$ (this fluid is equivalent to a cosmological term -the Einstein equation in this case is $G_{\mu\nu} + \Lambda g_{\mu\nu} = 8\pi G T_{\mu\nu}$- which is just a constant term in Friedmann equations). So if we consider that the Universe is made with matter, radiation, a cosmological term (so a fluid with $\omega = -1$) and has a curvature, we have that (6) is the so called consistent relation:

$$\Omega_K + \Omega_\Lambda + \Omega_M + \Omega_R = 1 \tag{10}$$

Since $a \propto t^{\frac{2}{3}\frac{1}{1+\omega}}$ and $k \simeq 0$, we have that at the beginning the Universe was dominated by radiation ($\Omega_R > \Omega_M$), then there was a matter-dominated period (from the time at which $\Omega_R(t_{eq}) = \Omega_M(t_{eq})$ and it turns out that $t_{eq} = 50.000$ years) and after that from $z_\Lambda = 0.44$ up to now the Universe is dominated by the cosmological term, that is the dark energy (z_Λ is so that $\Omega_\Lambda = \Omega_M(z_\Lambda)$ and the fact that z_Λ is very close to our present time it is quite strange because it means that acceleration has begun very recently: this is the so called cosmic coincidence problem). The flat ΛCDM model (which has proven able to describe a wide variety of observations, from the low to the high redshift Universe) considers the Universe as made up with two dominants components: the Cold Dark Matter (CDM) and the Cosmological Constant (Λ). In this cosmological model, equation (10) is therefore:

$$\Omega_\Lambda + \Omega_M = 1 \tag{11}$$

As we will see in next sections, equation (11) is what is used by DES in order to further test the ΛCDM model and try to constrain the dark energy density.

Now we want to work on the second Friedmann equation, so equation number (4), and our aim is to understand why there should be something missing in our acknowledge of the Universe, whether it is something wrong in General Relativity at cosmological scales or a new kind of energy that dominates the Universe at the present time -dark energy-. We note that equation (4) relates the Universe acceleration to its density (ρ) and pressure (p). We define the deceleration parameter as:

$$q = -\frac{\ddot{a}}{aH^2} = -\frac{\ddot{a}a}{\dot{a}^2} \tag{12}$$

Therefore if $q > 0$ it means that the Universe is decelerating, while if $q < 0$ the Universe is accelerating. With this definition and using the equation of state, equation (4) becomes:

$$q = \frac{\Omega}{2}(1 + 3\omega) \tag{13}$$

What discriminates between an accelerating or decelerating Universe is therefore ω ($\Omega > 0$ by definition). It turns out that the Universe is accelerating if $\omega < -\frac{1}{3}$. But where is the point? The point is that for Cold Dark Matter $\omega = 0$ and so $q = \frac{1}{2}\Omega > 0$ then we have deceleration and for radiation $\omega = \frac{1}{3}$ then $q = \Omega > 0$ and so deceleration again. As a consequence if we can measure experimentally q and we observe a $q < 0$, this cannot be explained neither by a matter-dominated Universe nor by a radiation-dominated one: there should be something more and unknown. Actually this is what happens. Indeed through high redshift measurements it is possible to have an experimental esteem of q and it has been observed that $q_0 < 0$, where q_0 is the

value of q at the present time. To be more precise, we can measure q by using Hubble law at the second order (if we are at high redshift so that we can appreciate also the term in z^2):

$$H_0 d_L = z + \frac{1}{2}(1 - q_0)z^2 \tag{14}$$

where d_L is the luminosity distance which is define as:

$$d_L = a(t_0) r_S (1 + z) \tag{15}$$

r_s is the distance coordinate from the observer to the source. Thus now we have the following problem: experimentally $q < 0$ and the only way to make it possible inside General Relativity is that the Universe is dominated by a fluid with an equation of state parameter $\omega < -\frac{1}{3}$, but:

- matter has $\omega = 0$
- radiation has $\omega = \frac{1}{3}$

So what is going on here? And what could be the possible solutions to this problem? There are two different answers to these questions.

1. We have to modify General Relativity so that it explains the acceleration: in this case we assume that General Relativity is incomplete at cosmological scales but, since there are experimental proofs of this theory, the correction should be very small. One possibility is that we can modify the action in the following way:

   $$S = \frac{1}{16\pi G} \int d^4x \sqrt{-g} F(\phi) R \tag{16}$$

   where ϕ is a scalar field and the difference with the typical action is the $F(\phi)$ factor. Another possibility is that we can introduce a mass term for gravitons, that fence gravity at large distances.

2. We assume that General Relativity works also at cosmological scales and that there is something beyond Standard Model. We introduce a new kind of matter, in particular the most accredited solution is a scalar field with $\omega < -\frac{1}{3}$. For instance if we have the lagrangian

   $$\mathcal{L} = \frac{1}{2}\partial_\mu Q \partial^\mu Q + V(Q) \tag{17}$$

   then energy-momentum tensor is

   $$T_{\mu\nu} = \partial_\mu \phi \partial_\nu \phi - g_{\mu\nu}(\frac{1}{2}\partial_\sigma \phi \partial^\sigma \phi + V(\phi)) \tag{18}$$

   and so if $\dot{Q} << V(Q)$ then we have that

   $$\omega = \frac{p}{\rho} \longrightarrow -\frac{V(Q)}{V(Q)} = -1 \tag{19}$$

   In this way we have obtained what we were looking for: a new kind of matter (a scalar field Q whose nature is unknown) that has $\omega = -1$, and can therefore be a perfect candidate for the cosmological term and so it could be what dominates the Universe at the present time. The problem of the cosmological constant is that if we look at the vacuum energy density associated to the zero-point fluctuations of quantum fields (that contributes to the cosmological constant) we see that it is much larger than the critical density of the Universe. This is not in agreement with the fact that the Universe can be considered flat (from observations it has been seen that the curvature k is $\simeq 0$). Moreover it turns out also that the vacuum energy density is much greater than ρ_Λ and of course this is a big problem too.

To summarize: observations have proven the Universe acceleration which isn't predicted in our theories (General Relativity plus the fact the Universe is composed by cold dark matter and

radiation). This means that or General Relativity has to be modified (and in this case the cosmological model continues to include only cold dark matter and radiation) or a new kind of matter with $\omega < -\frac{1}{3}$ has to be introduced (its energy density is what we call dark energy) and in the ΛCDM model discussed before it is the cosmological term (it has $\omega = -1$).

2 Dark Energy Survey Y1

The Dark Energy Survey is a six-year survey (August 2013-January 2019) that mapped 5000 deg^2 of the southern sky in five broadband filters (g,r,i,z,Y) using the 570 megapixel Dark Energy Camera, located on the 4m Blanco telescope at the Cerro TololoInter-American Observatory. The aim of the survey is to further test the ΛCDM model -because despite its success in low and high redshift observations, there is the lack of a fundamental theory that can connect the cold dark matter and the cosmological constant with the rest of physics- as well as the mechanism that drives the cosmic acceleration: be it a cosmological constant, some form of dark energy (so in general a fluid with $\omega < -\frac{1}{3}$ and not needs $\omega = -1$), or a modification of General Relativity. In this work we focus on data collected by DECam during the Year 1 (Y1) observational season, running from 31 August 2013 to 9 February 2014, which covers $\sim$ 1800 deg^2 of the southern sky. The final DES Y1 footprint -we are talking about final because some regions of the observed sky were excluded from the analysis- is shown in Figure 1: the upper panel is the Stripe 82 region (116 deg^2) while the lower one is the SPT region (1321 deg^2). The analysis of DES Y1 is done with galaxy clusters, which are the largest objects bounded together by gravity in the Universe ($10^{14} - 10^{15}$ solar masses) and are one of the key probes of dark energy measurements. The photometric cluster finder used in DES Y1 is redMaPPer (red-sequence Matched-filter Probabilistic Percolation cluster finder). This algorithm creates an optically-selected catalog by identifying galaxy clusters as overdensities of red-sequence galaxies. The goal of the survey is reached by simultaneously constraining cosmology and the observable-mass relation through cluster abundances and weak lensing. We are talking about observable-mass relation because it is not possible to directly estimate a cluster mass, but we need a mass proxy. The mass proxy chosen in DES Y1 is richness λ: it is the number of red galaxies in a cluster; to be more precise it is the sum of the membership probability of red galaxies in the cluster. Only red galaxies are considered in richness for three reasons: they have a better photometric redshift (so it is possible to be more sure that they are in the cluster); they have been in a cluster for a longer period than the blue galaxies and they are more massive than blue galaxies.

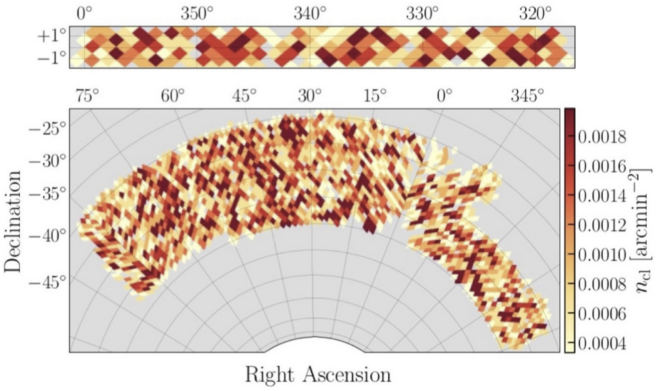

Figure 1: DES Y1 footprint, which is composed by two non-contiguous regions: the Stripe 82 region (116 deg^2; upper panel) and the SPT region (1321 deg^2; lower panel).

Galaxy Cluster: SMACS 0723

Image credit: NASA, ESA, CSA, and STScI, James Webb Space Telescope, 2022 (infrared)

Galaxy Cluster: Abell 370

Image Credit: NASA, ESA, Hubble, 2019 (visible)

Figure 2: Gravitational Lensing images.

After having the richness value, through weak lensing it is possible to calibrate the richness-mass relation and it turns out that it is a convolution of a Poisson and a Gaussian distribution. Gravitational lensing induces distortions in the images of back-ground source galaxies (as we can see in Figure 2) and it is a very powerful resource since it is sensible without differences both to baryonic and dark matter (galaxies and clusters are just seen as dark matter halos of differing masses) [see Appendix A for dark matter problem]. In the limit of weak gravitational lensing, the distorted images of the source are characterized by the reduced shear g:

$$g \equiv \frac{\gamma}{1-\kappa} \tag{20}$$

where γ is the shear and κ is the convergence. The gravity of a localized mass distribution, such as a galaxy cluster, induces positive shear along the tangential direction with respect to the center of the overdensity. It is possible to find the azimuthally averaged tangential shear γ_T (which is the observable) at the projected radius R:

$$\gamma_T = \frac{\Sigma(<R) - \Sigma(R)}{\Sigma_{crit}} \equiv \frac{\Delta\Sigma(R)}{\Sigma_{crit}} \tag{21}$$

where $\Sigma(R)$ is the line-of-sight surface mass density at R; $\Sigma(<R)$ represents the surface mass density within projected radius R and Σ_{crit} is the critical surface mass density, which characterize the geometry of the source-lens system that modulates the amplitude of the induced shear signal. The definition of Σ_{crit} is:

$$\Sigma_{crit}(z_s, z_l) = \frac{c^2}{4\pi G}\frac{D_s}{D_l D_{ls}} \tag{22}$$

where D_l, D_s and D_{ls} are respectively the angular diameter distance to the lens, to the source and between the lens and the source; while z_s and z_l are the source and the lens redshift. The

differential surface density is defined as:

$$\Sigma(< R) = \frac{2}{R^2} \int_0^R dR' \; R' \; \Sigma(R') \qquad (23)$$

So we need to understand now what the surface density is. Its definition is:

$$\Sigma(R) = \Omega_M \rho_{crit} \int_{-\infty}^{\infty} dz \; \xi_{hm}(\sqrt{R^2 + z^2}) \qquad (24)$$

where ξ_{hm} is the halo-matter correlation function, which is the tendency to find matter near halos. Correlation functions are what the question now moves on. Cluster density profiles are closely related to the halo-matter correlation function:

$$\rho(r) = \Omega_M \rho_{crit}(1 + \xi_{hm}) \qquad (25)$$

This equation means that the average density of halo at some distance r from the center of the halo is proportional to the mean density of the Universe and the halo-matter correlation function. The 3-d density profile that we use in this work is the NFW profile, which has been found through N-body simulations with the intent of investigating the structure of dark halos in the Standard Cold Dark Matter cosmology:

$$\rho_{nfw}(r) = \frac{\Omega_M \rho_{crit} \delta_C}{(\frac{r}{r_s})(1 + \frac{r}{r_s})^2} \qquad (26)$$

where r_s is the scale radius and δ_C is the normalization. This ρ_{nfw}-predicted structure of galaxy clusters is consistent both with X-ray observations of the intra-cluster medium and with the presence of giant gravitationally lensed areas. Then the corresponding correlation function is:

$$\xi_{nfw}(r) = \frac{\rho_{nfw}(r)}{\Omega_M \rho_{crit}} - 1 \qquad (27)$$

We notice that the NFW profile describes the 1-halo density of halos, that is the density of a halo within its boundary. However, halos tend to be found near other halos and for this reason the average density of halos should also have a 2-halo term. As we move far from the center of a halo the halo-matter correlation function becomes the 2-halo term:

$$\xi_{hm}(r >> r_s) = \xi_{2-halo}(r) \qquad (28)$$

Since halos are biased tracers of the matter density field, the two-halo correlation function is:

$$\xi_{2-halo}(r, M) = b(M)\xi_{mm}(r) \qquad (29)$$

where b(M) is the bias (a function of mass) and ξ_{mm} is the matter auto-correlation function (so it describes the average density of matter). So now, knowing that at small scales the correlation function follows the 1-halo term while at large scales it follows the 2-halo term, we can understand what is the ξ_{hm} expression:

$$\xi_{hm}(r, M) = sum(\xi_{1-halo}, \xi_{2-halo}) \qquad (30)$$

Now we have understood all the terms that appear in equation (21), that is the expression of the experimental weak lensing observable that we have. Next goal is to understand how DES Y1 data vector (Table 1 and Table 2) is constructed. The steps to follow in order to do that, are:

- measure redshift through spectroscopy;
- measure richness;
- create a redshift and richness binning scheme in order to achieve high signal-to-noise measurements of the weak lensing profile of galaxy clusters;
- count the number of galaxy clusters and compute their masses in said bins.

λ	$z \in [0.2, 0.35)$	$z \in [0.35, 0.5)$	$z \in [0.5, 0.65)$
$[20, 30)$	762 (785.1) $\pm$ 54.9 $\pm$ 8.2	1549 (1596.0) $\pm$ 68.2 $\pm$ 16.6	1612 (1660.9) $\pm$ 67.4 $\pm$ 17.3
$[30, 45)$	376 (388.3) $\pm$ 32.1 $\pm$ 4.5	672 (694.0) $\pm$ 38.2 $\pm$ 8.0	687 (709.5) $\pm$ 36.9 $\pm$ 8.1
$[45, 60)$	123 (127.2) $\pm$ 15.2 $\pm$ 1.6	187 (193.4) $\pm$ 17.8 $\pm$ 2.4	205 (212.0) $\pm$ 17.1 $\pm$ 2.7
$[60, \infty)$	91 (93.9) $\pm$ 14.0 $\pm$ 1.3	148 (151.7) $\pm$ 15.7 $\pm$ 2.2	92 (94.9) $\pm$ 14.2 $\pm$ 1.4

Table 1: Number of galaxy clusters in the DES Y1 redMaPPer catalog for each richness and redshift bins. Each entry takes the form $N(N) \pm \Delta N\ stat \pm \Delta N\ sys$, where: the numbers between parenthesis correspond to the number counts corrected for the miscentering bias factors; the first error bar corresponds to the statistical uncertainty in the number of galaxy clusters in that bin, while the second error bar is the systematic error.

λ	$z \in [0.2, 0.35)$	$z \in [0.35, 0.5)$	$z \in [0.5, 0.65)$
$[20, 30)$	$14.036 \pm 0.032 \pm 0.045$	$14.007 \pm 0.033 \pm 0.056$	$13.929 \pm 0.048 \pm 0.072$
$[30, 45)$	$14.323 \pm 0.031 \pm 0.051$	$14.291 \pm 0.031 \pm 0.061$	$14.301 \pm 0.041 \pm 0.086$
$[45, 60)$	$14.454 \pm 0.044 \pm 0.050$	$14.488 \pm 0.044 \pm 0.065$	$14.493 \pm 0.056 \pm 0.068$
$[60, \infty)$	$14.758 \pm 0.038 \pm 0.052$	$14.744 \pm 0.038 \pm 0.052$	$14.724 \pm 0.061 \pm 0.069$

Table 2: Mean mass estimates for DES Y1 redMaPPer galaxy clusters in each richness and redshift bins. The reported quantities are $log_{10}(M)$. The first error bar refers to the statistical error, while the second one is the systematic uncertainty.

Source of systematic	Y1 Amplitude Uncertainty
Shear measurement	1.7%
Photometric redshifts	2.6%
Modeling systematics	0.73%
Cluster triaxiality	2.0%
Line-of-sight projections	2.0%
Membership dilution + miscentering	0.78%
Total Systematics	4.3%
Total Statistical	2.4%
Total	5.0%

Table 3: Sources of systematics uncertainties in the cluster mass calibration with the relative amplitudes in DES Y1 analysis.

Talking about systematic uncertainties, we have that the ones associated to cluster counts are well understood: the covariance matrix of cluster counts is due to Poisson noise, sample variance and cluster miscentering. Sources of systematic errors in the cluster mass calibration are more difficult, since we have to deal with many different effects. In Table 3 there is a list of all those systematics uncertainties, and here we are doing also an explanation of them:

- Shear multiplicative bias: there could be an over- or under- estimation of gravitational shear (mean tangential ellipticity of lensed galaxies);
- Redshift systematic uncertainties;
- Modeling systematics: inaccuracies in the halo-mass correlation function model;
- Cluster triaxiality: dark matter halos have triaxial shapes and so if we have a cluster sample which is dominated by clusters with major axes aligned along the line-of-sight, the lensing signal will be boosted rel-

ative to the prediction based on spherically symmetric halos;

- Line-of-sight projections: there could be changes in the cluster lensing signal and in richness due to matter and galaxies projected along the line-of-sight;
- Miscentering: redMaPPer doesn't always correctly center clusters.

In Figure 3 we can see the results of DES Y1. The shaded areas are the observed cluster number counts (on the left) and mean cluster masses (on the right), while the dots are the best-fit model of the same quantities. They are plotted as functions of richness for each of the three redshift bins. The bottom panel shows the residual between the data and DES Y1 best-fit model. Then in Table 4 we report the model parameters and the parameters constraints obtained from the joint analysis of redMaPPer DES Y1 cluster abundance and weak-lensing mass estimates (notice that the matter density obtained is $\Omega_M = 0.179^{+0.031}_{-0.038}$).

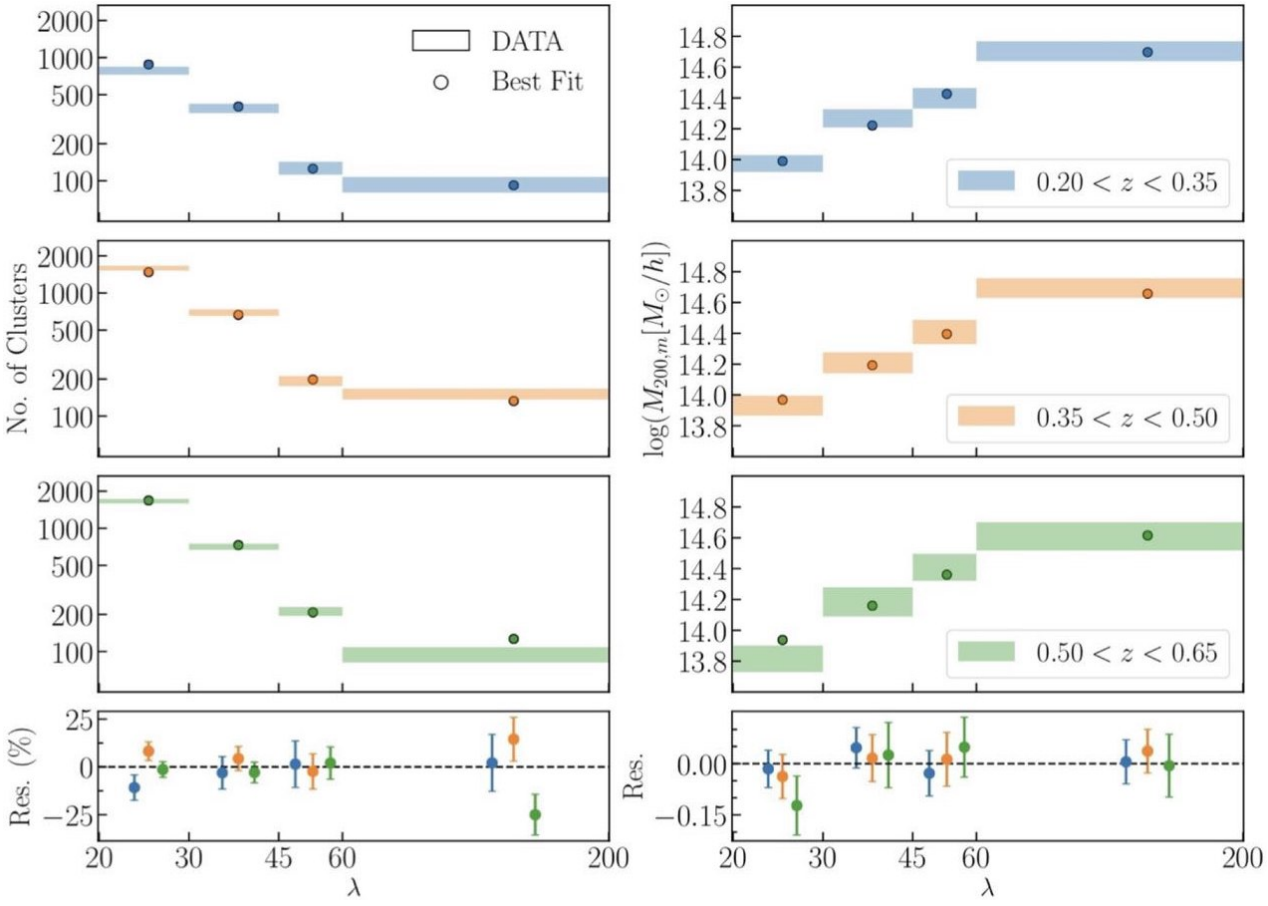

Figure 3: Observed (shaded areas) and best-fit model (dots) for the cluster number counts (left) and the mean cluster masses (right) as a function of richness for each of the three redshift bins. The bottom panel shows the residual between data and the best-fit model (points are slightly displaced along the x axis to avoid overcrowding).

Parameter	Description	Prior	Posterior
Ω_m	Mean matter density	$[0.0, 1.0]$	$0.179^{+0.031}_{-0.038}$
$\ln(10^{10}A_s)$	Amplitude of the primordial curvature perturbations	$[-3.0, 7.0]$	4.21 ± 0.51
σ_8	Amplitude of the matter power spectrum	–	$0.85^{+0.04}_{-0.06}$
$S_8 = \sigma_8(\Omega_m/0.3)^{0.5}$	Cluster normalization condition	–	$0.65^{+0.04}_{-0.04}$
$\log M_{min}[\mathrm{M}_\odot/h]$	Minimum halo mass to form a central galaxy	$(10.0, 14.0)$	11.13 ± 0.18
$\log M_1[\mathrm{M}_\odot/h]$	Characteristic halo mass to acquire one satellite galaxy	$\log(M_1/M_{\min}) \in [\log(10), \log(30)]$	12.37 ± 0.11
α	Power-law index of the richness–mass relation	$[0.4, 1.2]$	0.748 ± 0.045
ϵ	Power-law index of the redshift evolution of the richness–mass relation	$[-5.0, 5.0]$	-0.07 ± 0.28
σ_{intr}	Intrinsic scatter of the richness–mass relation	$[0.1, 0.5]$	< 0.325
s	Slope correction to the halo mass function	$\mathcal{N}(0.047, 0.021)$	–
q	Amplitude correction to the halo mass function	$\mathcal{N}(1.027, 0.035)$	–
h	Hubble rate	$\mathcal{N}(0.7, 0.1)$	0.744 ± 0.075
$\Omega_b h^2$	Baryon density	$\mathcal{N}(0.02208, 0.00052)$	–
$\Omega_\nu h^2$	Energy density in massive neutrinos	$[0.0006, 0.01]$	–
n_s	Spectral index	$[0.87, 1.07]$	–

Table 4: Model parameters and parameters constraints from the joint analysis of redMaPPer DES Y1 cluster abundance and weak-lensing mass estimates. In the third column there are the model priors ($\mathcal{N}(\mu, \sigma)$ stands for a Gaussian prior). The fourth column lists the modes of the 1-d marginalized posterior along with the 1-σ errors. Parameters without a quoted value are those for which the marginalized posterior distribution is the same as their prior.

The ΛCDM model considers the following parameters: $\Omega_\Lambda \simeq 0.7$, $\Omega_M \simeq 0.3$ (while $\Omega_B \simeq 0.05$, here Ω_B is the baryonic matter density [see Appendix A]) and $\Omega_R \simeq \Omega_K \simeq 0$. Thus we have that the Ω_M value obtained by DES Y1 ($\Omega_M = 0.179^{+0.031}_{-0.038}$) is not compatible with the ΛCDM model expected value (the same stands for Ω_Λ since we can use equation (11) assuming flat ΛCDM cosmological model). Instead, σ_8 value obtained ($\sigma_8 = 0.85^{+0.04}_{-0.06}$) is comparable with the one expected: σ_8 is the rms value of matter density fluctuations in a sphere of radius $8h^{-1}Mpc$ (where $h \simeq 0.75$) with an expected value of 0.81. Because of the low Ω_M value, we have a surprisingly low value for $S_8 = \sigma_8(\frac{\Omega_M}{0.3})^{0.5}$: $S_8 = 0.65 \pm 0.04$. In Figure 4 there is a comparison between DES Y1 posteriors on S_8 and the ones derived from a variety of different experiments: the tension in S_8 of DES Y1 posterior relative to the other low-redshift probes is ranging from 1.5σ to 2.5σ; if we compare it to Planck CMB result then the tension in S_8 reaches 4.0σ.

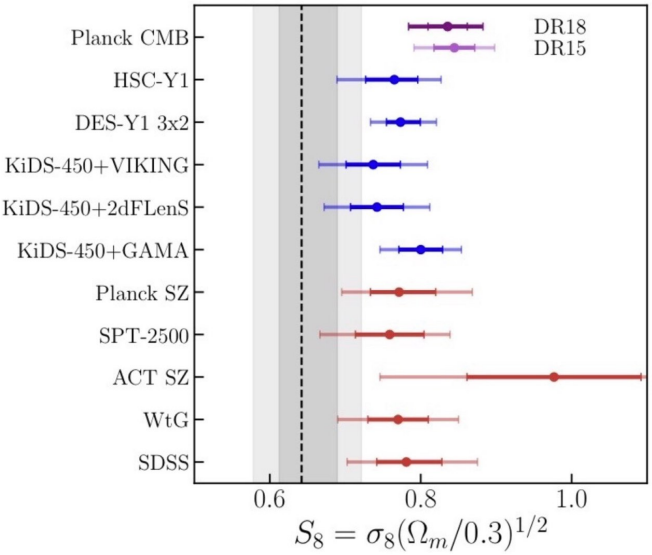

Figure 4: Comparison of the 68% (dark) and 95% (light) confidence level constraints on S_8 derived from DES Y1 analysis (shaded gray area) and other experiments from literature. Red error bars are for cluster abundance analyses, blue ones for weak lensing and galaxy clustering analyses and purple for the CMB constraint.

If we naively combine all the nine low-redshift experiments assuming they are mutually independent, the DES Y1 cluster result has 2% probability of being a statistical fluctuation around their mean.

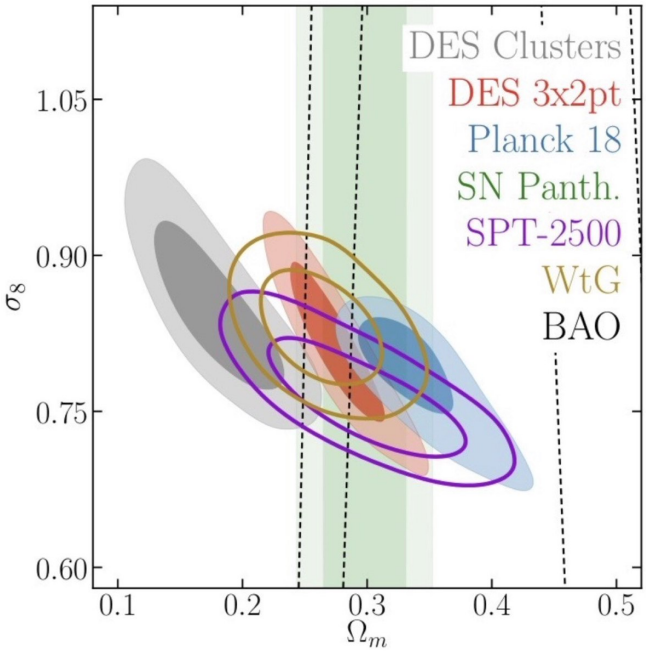

Figure 5: Comparison of the 68% (dark) and 95% (light) confidence contours in the $\sigma_8 - \Omega_M$ plane derived from DES Y1 cluster counts and weak-lensing mass calibration (gray contours) with other constraints from literature.

In Figure 5 there is a comparison between the 68% and the 95% confidence regions in the $\sigma_8 - \Omega_M$ plane derived from different experiments. This figure makes clear that the S_8 tension is due to the low value of Ω_M obtained by DES Y1. Because of the fact that all the other cosmological probes have obtained significantly higher values for Ω_M, and also from the fact that DES 3x2pt, that is based on the same data of DES Y1 (but uses galaxies instead of clusters in the analysis and uses three two-points correlation functions: cosmic shear, galaxy clustering, galaxy-galaxy lensing), obtains comparable cosmological constraints to the ones of all the other probes, we can think that there could be the presence of unexpected systematics or physics in DES Y1 analysis. A possibility that has been explored is whether these tensions could be reduced by considering a different cosmological model. An analysis with ωCDM model (so considering the equation of state parameter of dark energy $\omega \in [-2, -\frac{1}{3}]$) was done, and it turned out that it doesn't imply any improvement in the agreement between DES clusters and the remaining data sets.

3 Selection Effect Bias

In order to try to understand if there are possible unmodeled systematics in the data, we compare the cluster masses or the number count of clusters (so our data vector) with the same quantities predicted with the respective complementary data set combined with DES 3x2pt priors: Figure 6. The shaded areas are the observed data vector (of number counts on the left and of masses on the right), while dots are the predicted quantities: on the left we have the predicted number counts estimated using the combination of the observed weak-lensing masses and DES 3x2pt cosmology, while on the right there are the predicted masses obtained through the number counts data and DES 3x2pt cosmological priors. Focusing on the left part of the graph, we can notice that if we assume that the recovered cluster masses and 3x2pt cosmology are right, then the redMaPPer catalog should be highly incomplete. In particular it should be $\sim 50\%$ incomplete at low richness and between $10\% - 40\%$ incomplete at the highest richness bin. The point is that such a large incompleteness, especially at high richness, is unlikely: the redMaPPer cata-

logs have been extensively vetted over the years and for instance 100% of the SPT and Planck SZ clusters within the DES Y1 footprint and below redshift 0.65 are detected by redMaPPer. Since DES 3x2pt cosmology is comparable with all the other surveys, we can think the problem is on the estimation of weak-lensing masses. The right panels of Figure 6 compares the cluster masses predicted by DES Y1 analysis to the ones estimated through the observed cluster counts and 3x2pt cosmology. We see weak-lensing masses are low relative to the predicted ones: the difference is $\sim 30-40\%$ in the lowest richness bins and $\sim 10\%$ in the highest bins. We interpret all these differences as due to DES Y1 masses esteems: the analysis is limited by the accuracy of cluster mass calibration. Therefore we focus on the cluster's excess surface density profile $\Delta\Sigma$ (equation (21)) which is the cluster lensing observable (to be more precise it is γ_T).

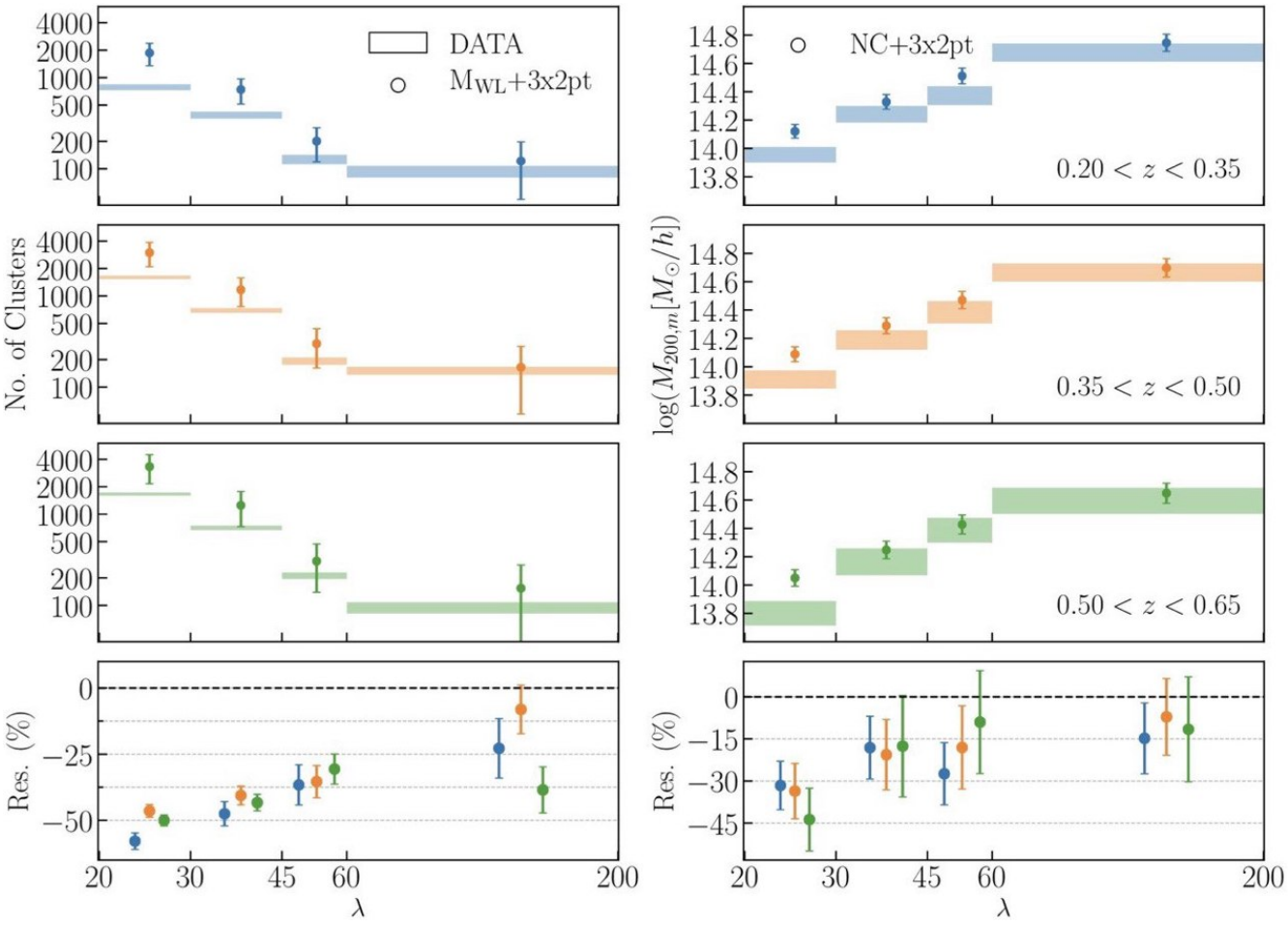

Figure 6: Comparison of the observed data vectors (shaded areas) with the number counts predicted from the combination of weak-lensing mass estimates and DES Y1 3x2pt cosmology (left panel) and mean masses predicted from the combination of Y1 number counts data and DES 3x2pt cosmology (right panel). The lower panel shows the percent residual of the data vector to the prediction.

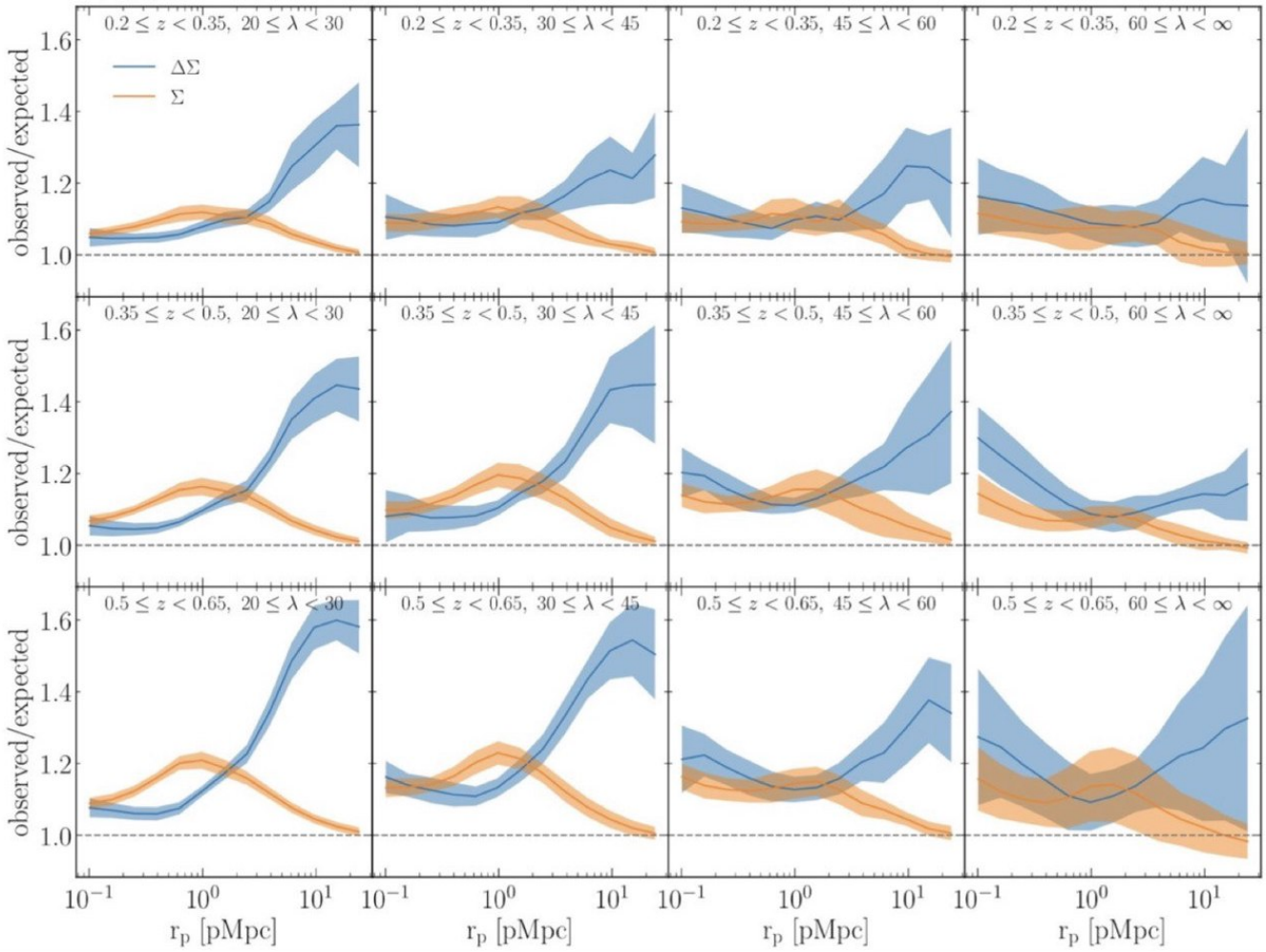

Figure 7: Ratio between the signal from a richness-selected sample (observed) and the signal expected from the halo mass probability distribution function (expected) for different richness-redshift bins. For Σ at approximately 1 pMpc there is a peak and then the bias vanishes at large scales. The bias for $\Delta\Sigma$ is non-vanishing at large scales because $\Delta\Sigma$ at each r_p contains the information of Σ from $r < r_p$. The bias in $\Delta\Sigma$ can be as high as 20 to 60 % at large r_p.

In Figure 7 there are plots of the ratio $\Delta\Sigma_{observed}/\Delta\Sigma_{expected}$ in richness-redshift bins, and we can see that the profile it is not a straight horizontal line at 1. We can attribute this difference to a selection bias: optically identified galaxy clusters are prone to selection effects that can bias the weak lensing mass calibration. The selection effect induces correlation between the weak lensing signal and cluster richness at a given cluster halo mass. As a consequence the lensing signal is biased compared with what we would expect from the halo-mass probability distribution function. We can analytically model the selection bias by assuming that $ln\lambda$ and $ln\Sigma$ follow a bivariate Gaussian distribution. We assume that this joint probability distribution

function has a mean:

$$(\langle ln\lambda|M\rangle \, , \, \langle ln\Sigma|M\rangle \,) \tag{31}$$

and a covariance matrix:

$$\mathcal{C} = \begin{pmatrix} \sigma^2_{ln\lambda} & r\sigma_{ln\lambda}\sigma_{ln\Sigma} \\ r\sigma_{ln\lambda}\sigma_{ln\Sigma} & \sigma^2_{ln\Sigma} \end{pmatrix} \tag{32}$$

where r is the correlation coefficient (so if there is not correlation between Σ and λ then $r = 0$), $\sigma_{ln\Sigma}$ and $\sigma_{ln\lambda}$ are the standard deviations of the two observables at a given mass. Therefore the conditional probability distribution of $ln\Sigma$ given $ln\lambda$ corresponds to a Gaussian distribution with the mean:

$$\langle ln\Sigma|ln\lambda, M\rangle = \langle ln\Sigma|M\rangle + r\sigma_{ln\Sigma}\frac{ln\lambda - \langle ln\lambda|M\rangle}{\sigma_{ln\lambda}} \tag{33}$$

The last term in equation (33) describes the selection bias associated with cluster lensing (if there is not correlation then $r = 0$ and so we don't have that term).

We want to include the selection effect in DES Y1 analysis by doing a simultaneous likelihood between cosmology, richness-mass relation and the selection effect. So we want to empirically design a functional form for the $\Delta\Sigma$ profile in Figure 7 and to obtain that model parameters values through the simultaneous likelihood at each step of the Markov Chain Monte Carlo (DES Y1 analysis is driven by MCMC chains). The goal of this new analysis is to see whether the final cosmological constraints will be the same of the previous analysis (and so we will still obtain $\Omega_M \simeq 0.18$) or if we will have a Ω_M value closer to the ones that are in literature. Our model for the $\Delta\Sigma_{observed}/\Delta\Sigma_{expected}$ profile shown in Figure 7 is:

$$\frac{\Delta\Sigma_{observed}}{\Delta\Sigma_{expected}} = a\ ln^2R + b\ lnR + c \tag{34}$$

with

$$a = a_0 + \left(\frac{\lambda}{30}\right)^{\alpha_a} + \left(\frac{1+z}{1.3}\right)^{\beta_a} \tag{35}$$

$$b = b_0 + \left(\frac{\lambda}{30}\right)^{\alpha_b} + \left(\frac{1+z}{1.3}\right)^{\beta_b} \tag{36}$$

$$c = c_0 + \left(\frac{\lambda}{30}\right)^{\alpha_c} + \left(\frac{1+z}{1.3}\right)^{\beta_c} \tag{37}$$

In this way we only have 9 free parameters which are shared across all richness-redshift bins.

4 CosmoSIS

If we want to understand how we can include selection effect in the analysis, we need to understand how DES Y1 analysis works. Code is run through CosmoSIS which connects together samplers (which decide how to explore a cosmological parameter space) with pipelines made from a sequence of modules (which calculate the steps needed to get a likelihood function). In order to include the selection bias in the analysis we thus have to write new modules, which include the model in equation (34), and to modify the likelihood. In Figure 8 there is a schematic example of a CosmoSIS run.

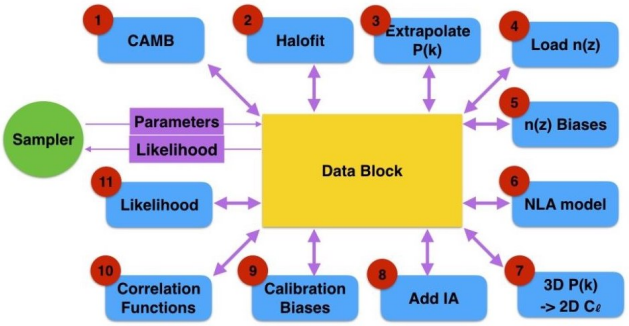

Figure 8: Schematic example of a CosmoSIS run.

- The green sampler generates parameters and sends them to the pipeline (which is just a sequence of modules, so it tells which modules and in which order have to be run). At the end of the run it gets a total likelihood back.
- The blue modules are independent codes run in the numbered sequence (the pipeline establishes the order). They each perform one step in the calculation of the likelihood. They are pieces of code in python, C, C++ or Fortran and needs to have two specially named functions in them: setup and execute. The setup function is run once at the beginning of the CosmoSIS process and the execute function is run at each step of the MCMC, so each time there are new input parameters for which the sampler wants the likelihood.
- The purple connections show that each module reads inputs from the DataBlock and then saves its results back to it.
- The yellow DataBlock acts like a big lookup table for data: it stores the initial parameters and then also the results from each module. Modules communicate via DataBlock.
- The blue Likelihood module computes a final likelihood value

In the DES Y1 analysis there is a module called *deltasigma* which computes Σ (the name of the module is misleading). So to include the selection bias in the analysis, we:

1. Write a new module called *finish* which computes $\Delta\Sigma$ starting from the Σ profile obtained in *deltasigma* module;
2. Write a second module called *parabola* where we multiply the $\Delta\Sigma$ profile obtained in the *finish* module for the parabola in equation (34);
3. Include these new modules in the pipeline;
4. Modify the *Likelihood* module so that we have a simultaneous likelihood for cosmology, richness-mass relation and the parabola model.

The final pipeline is shown in Figure 9.

```
[pipeline]
modules = consistency camb mf_tinker deltasigma SigmaCentY1MortCUDAScalarIntegrand SigmaMiscentY1MortCUDAScalarIntegrand
 NCCentY1MortCUDAScalarIntegrand NCMiscentY1MortCUDAScalarIntegrand finish parabola SigmaMort_Like
; The file to get cosmological and nuisance parameters
; from.
values = ${Y3_CLUSTER_CPP_DIR}/y1_rerun/values_y1_analysis.ini
likelihoods = SigmaMort_Like
extra_output = cosmological_parameters/sigma_8
quiet=T
debug=T
timing=T
```

Figure 9: Final pipeline, where there are also *finish* and *parabola* modules and where the Likelihood module (*SigmaMort Like*) has been modify in order to compute a simultaneous likelihood for cosmology, the observable-mass relation and the parabola parameters.

In order to make the *finish* module as fast as possible we have estimated the time needed to compute $\Delta\Sigma$ starting from Σ in different ways and using different toolkits, so that we can decide the best way to write the new module. Below there are the $\Delta\Sigma$ profiles obtained with the relative toolkit, way of computing and time of execution. In addition to all of them we have

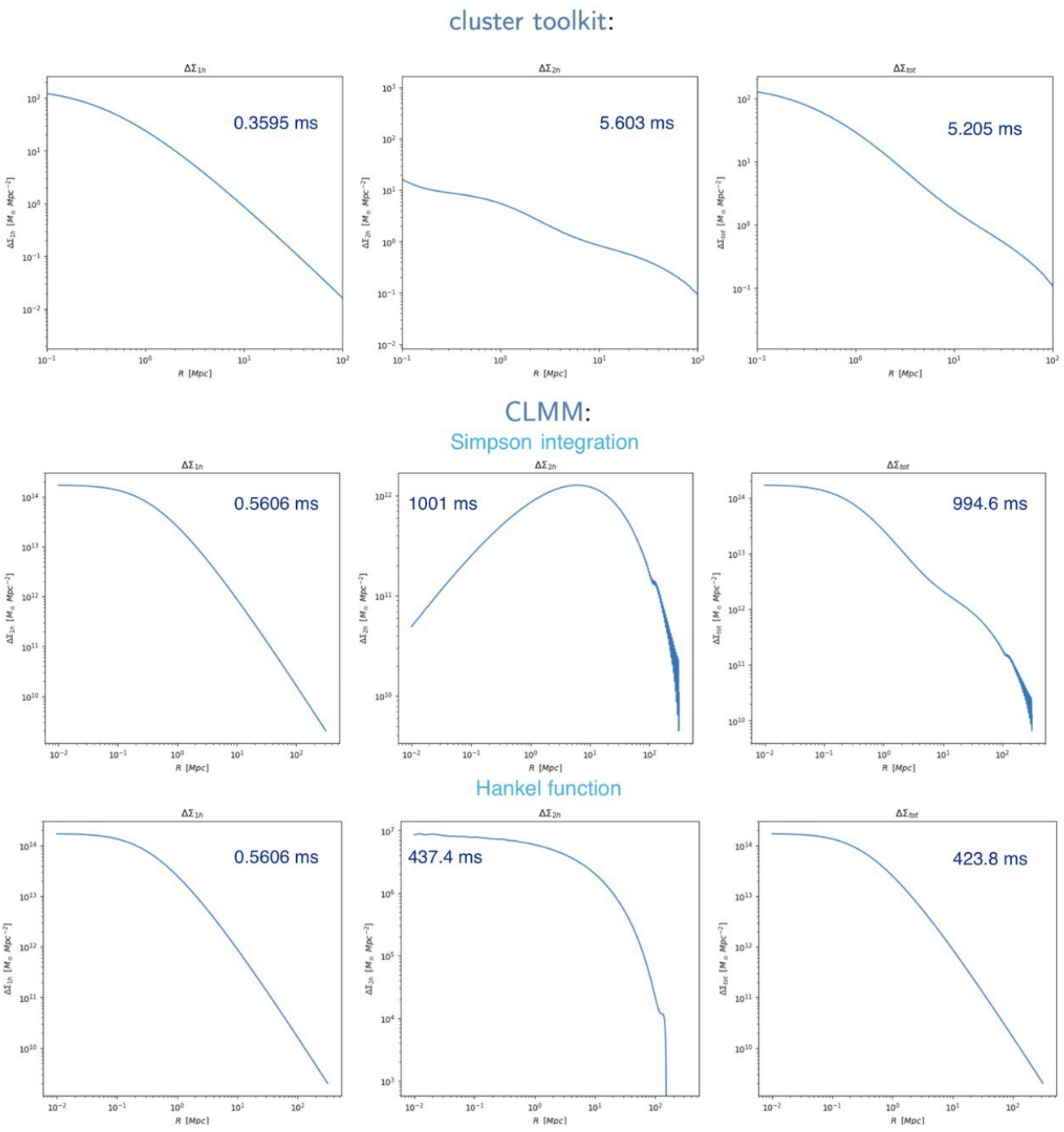

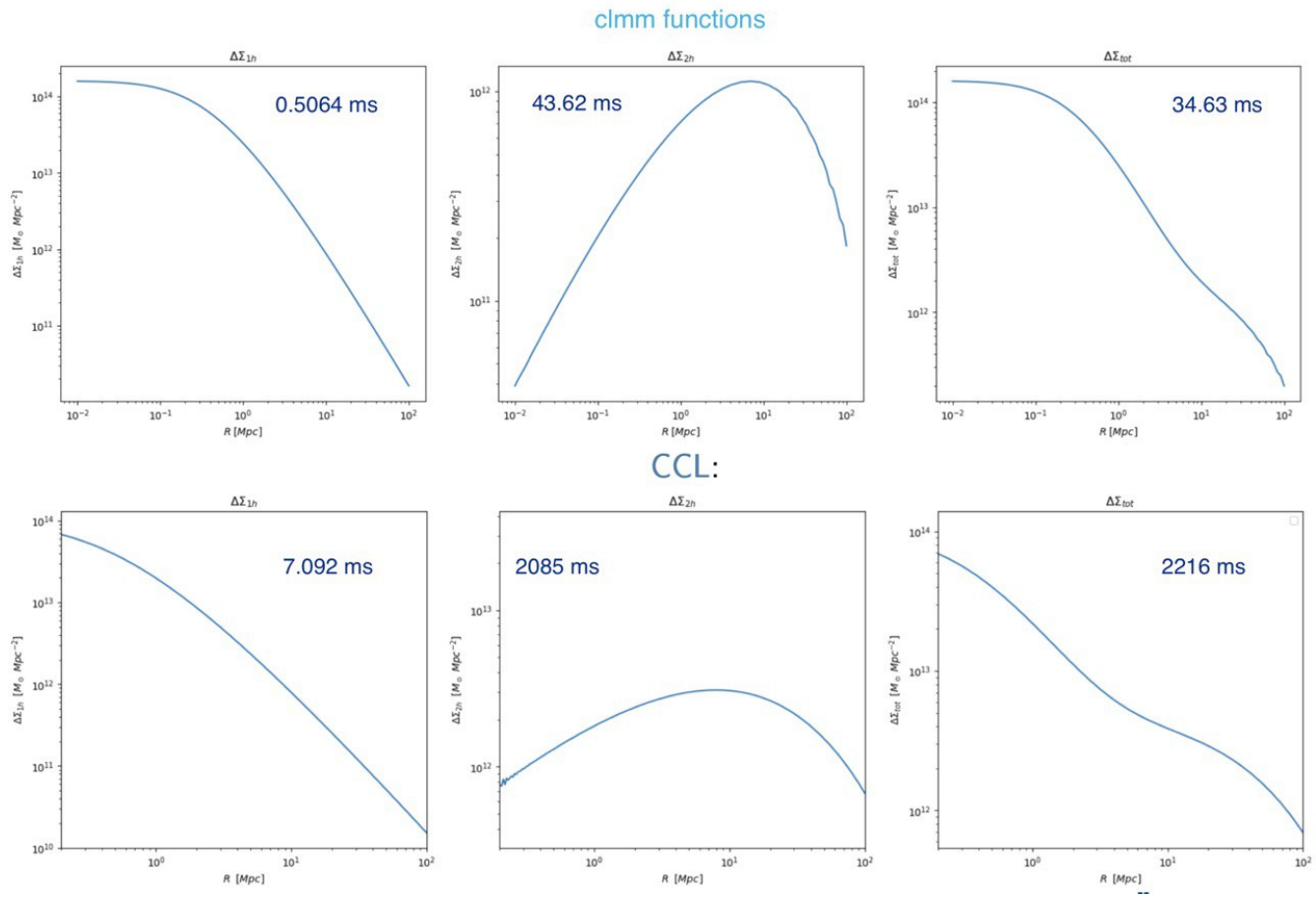

Figure 10: 1-halo ($\Delta\Sigma_{1h}$), 2-halos ($\Delta\Sigma_{2h}$) and total excess surface mass density profiles ($\Delta\Sigma_{tot}$) (which are computed in different ways) with the relative time of execution. From the top to the bottom they are computed: using cluster toolkit; using CLMM and a Simpson integration; using CLMM and the Hankel function; using CLMM and some clmm functions; using CCL. We notice the first method (so using cluster toolkit) is the fastest method to compute $\Delta\Sigma$ profiles among these ones.

also considered the possibility of computing $\Delta\Sigma$ by using the trapezoidal rule to calculate the integral in equation (23). It turns out that this last method is the best way to obtain the excess surface density and so we have used it in the *finish* module.

The next step is to run CosmoSIS with this new pipeline and see which are the new cosmological constraints obtained. If we will obtain $\Omega_M \sim 0.3$ then we will have to try to find theoretical explanations to the selection effect model, while if Ω_M still remains around 0.18, then we have to think about other possible systematics or effects to include in the analysis and also to consider the possibility that there could be something in cluster physics which is still not known.

References

[1] The DES Collaboration (2020), *Dark Energy Survey Year 1 Results: Cosmological Con-*

straints from Cluster Abundance and Weak Lensing, arXiv: 2002.11124

[2] Park et al. (2022), *Cluster Cosmology with anisotropic boosts: Validation of a novel forward modeling analysis and application on SDSS redMaPPer clusters*, arXiv: 2112.09059

[3] McClintock et al. (2018), *Dark Energy Survey Year 1 Results: Weak Lensing Mass Calibration of redMaPPer Galaxy Clusters*, arXiv: 1805.00039

[4] Wu et al. (2022) *Optical selection bias and projection effects in stacked galaxy cluster weak lensing*, arXiv: 2203.05416

[5] The DES Collaboration (2022), *Dark Energy Survey Year 3 Results: Cosmological Constraints from Galaxy Clustering and Weak Lensing*, arXiv: 2105.13549

[6] The DES Collaboration (2016), *The redMaPPer Galaxy Cluster Catalog from DES Science Verification Data*, arXiv: 1601.00621

[7] The CosmoSIS Team (2017), https://cosmosis.readthedocs.io/en/latest/intro/overview.html

[8] Tom McClintock (2017), https://cluster-toolkit.readthedocs.io/en/latest/

A Dark Matter Problem

From experiments we have that the matter density of the Universe is $\Omega_M \simeq 0.3$, while the baryonic one is $\Omega_B \simeq 0.05$: this is the so called dark matter problem. There are experimental hints for the existence of some new kind of matter beyond Standard Model or some needed modification in our laws (for example: gravitational lensing is observed even if we don't have a lens made with baryonic matter; the orbital velocities of stars don't decrease if we go far from the galaxy center but they reach a plateau). There are different possible explanations to the dark matter problem:

- Particles: there is a new kind of particle that is not included in Standard Model and which has an energy density equal to $0.3 - 0.05$. The classical solutions are WIMP (weakly interactive massive particles): they are cold relics which decouple when they are not relativistic (so the Boltzmann exponential in the Boltzmann equation is active) and that interact weakly (the cross section is $\sigma \sim 10^{-38} cm^2$). It is demonstrated they could perfectly explain the 0.3 value of Ω_M.

- MACHOS (massive astrophysical compact objects): they are almost planetary objects (candidates of baryonic dark matter) and have been searched through gravitational lensing. It has been demonstrated they cannot be a relevant portion of halos.

- Wave-like candidates: the classical ones are axions. Axions are pseudoscalar particles which are introduced also as a resolution to the strong CP problem.

- MOND (modified Newtonian dynamics): it is a modification of the Newton law, without any theoretical foundation. It states that

$$F = \begin{cases} ma & for \;\; a > a_0 \\ m\frac{a^2}{a_0} & for \; a < a_0 \end{cases} \tag{38}$$

with $a_0 \simeq 10^{-10}\, m\, s^{-2}$. This theory doesn't explain the Bullet Clusters (two

colliding clusters of galaxies) gravitational potential: the spatial offset of the center of the total mass from the center of the baryonic mass peaks cannot be explained with MOND.